Supporting information

Fe-mediated HER vs N_2RR: Exploring Factors that Contribute to Selectivity in $P_3^EFe(N_2)$ (E = B, Si, C) Catalyst Model Systems

Benjamin D. Matson and Jonas C. Peters*

Corresponding Author:
*jpeters@caltech.edu

Division of Chemistry and Chemical Engineering, California Institute of Technology, Pasadena, California 91125, United States

Table of Contents:

1. General Computational Details

All stationary point geometries were calculated using dispersion corrected DFT-D_3[1] with a TPSS functional,[2] a def2-TZVP basis set on transition metals and a def2-SVP basis set on all other atoms.[3] Calculations were performed, in part, using Xtreme Science and Engineering Discovery Environment (XSEDE) resources.[4] Calculations were performed on the full P_3^EFe scaffolds. Geometries were optimized using the NWChem 6.5 package or Orca 3.0.3 package.[5] All single point energy, frequency and solvation energy calculations were performed with the Orca 3.0.3 package. Frequency calculations were used to confirm true minima and to determine gas phase free energy values (G_{gas}). Single point solvation calculations were done using an SMD solvation model[6] with diethyl ether solvent and were used to determine solvated internal energy (E_{soln}). Free energies of solvation were approximated using the difference in gas phase internal energy (E_{gas}) and solvated internal energy ($\Delta G_{solv} \approx E_{soln} - E_{gas}$) and the free energy of a species in solution was then calculated using the gas phase free energy (G_{gas}) and the free energy of solvation ($G_{soln} = G_{gas} + \Delta G_{solv}$). All reduction potentials were calculated referenced to $Fc^{+/0}$ using the standard Nernst relation $\Delta G = -nFE^0$.

2. Fe–H Formation

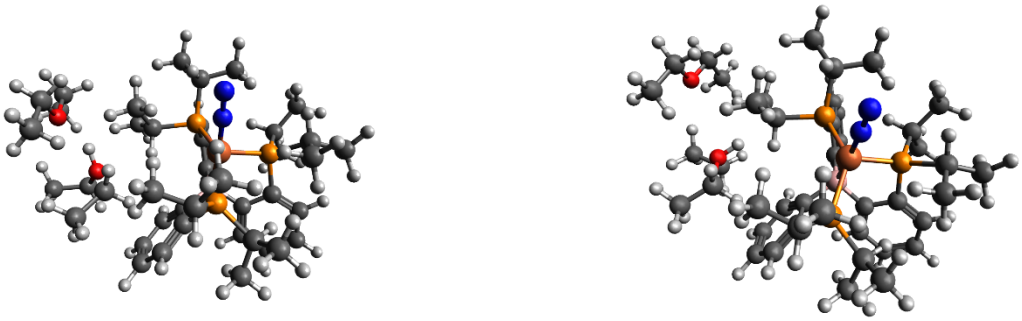

Figure S1. Structure of $P_3^BFeN_2^-$ + $(Et_2O)_2H^+$ immediately before (left) and after (right) dissociation of a Et2O moiety. The relaxed surface scan reveals little change in the $P_3^BFeN_2^-$ unit before Et_2O dissociation, indicative of the presence of a $(Et_2O)_2H^+ \leftrightarrows (Et_2O)H^+ + Et_2O$ pre-equilibrium.

3. BDFE Calculations

Bond dissociation free energies (BDFE) of X–H bonds were calculated in the gas-phase using a series of known reference compounds.[7] The free-energy difference between the H-atom donor/acceptor pair was calculated based on the thermochemical information provided by frequency calculations after structure optimizations using the procedure described in the general computational section. A linear plot of ΔG *vs* $BDFE_{lit}$ was generated to form a calibration curve (**Figure S1**). BDFE predictions were generated by application of the line of best fit to the calculated ΔG of the unknown species. Errors were calculated by application of the trend line to the calculated free-energies of known species and comparison to their literature BDFE value. Errors are reported as the average of $BDFE_{calc}$-$BDFE_{lit}$ (mean signed error, MSE = 0.0) and the average of the absolute values of $BDFE_{calc}$-$BDFE_{lit}$ (mean unsigned error, MUE = 1.3).

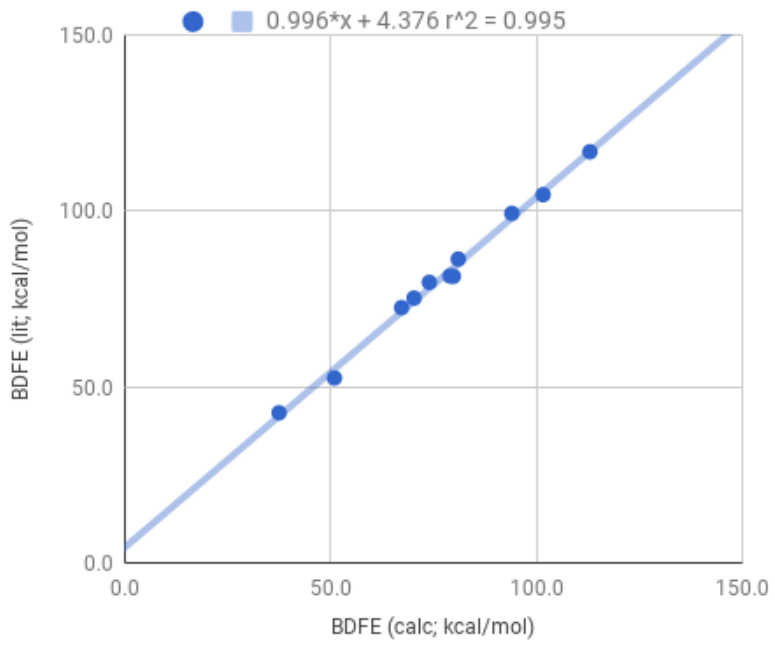

Figure S2. Plot of calculated BDFE vs literature BDFE. Line of Best fit shown with equation along with r^2 value.

Table S1. Summary of BDFEs used for calibration.

	ΔG (E-H)	**ΔG (E*)**	**ΔG_{calc}**	**$BDFE_{lit}$**	**Error**
$PhNH_2$	-287.4	-286.7	79.8	81.5	-2.4
NH_2NH_2	-111.8	-111.1	67.3	72.6	1.2
PhSH	-630.2	-629.5	70.3	75.3	0.9
PhH	-271.3	-270.7	79.0	81.6	-1.5
C_6H_6	-232.1	-231.4	101.6	104.7	-0.9
PhOH	-307.2	-306.6	74.0	79.8	1.7
NH_3	-56.5	-55.8	94.0	99.4	1.3
NHNH	-110.6	-110.0	51.0	52.6	-2.6
Me_2NH	-213.6	-212.9	81.0	86.4	1.3
NH_4 (+)	-56.8	-56.1	113.0	116.9	0.0
OOH	-150.8	-150.2	37.5	42.7	1.0
				MUE	1.4
				MSE	0.1

4. Approximation of $P_3^EFe(NNH_y)$ Radius

The radius of $P_3^EFe(NNH_y)$ was approximated by using the average molar volume of several relevant crystal structures to determine a radius assuming a spherical molecule.

Table S2. Volume and Calculated Radius of Previous Characterized P_3^EFe Species from XRD Data

	Volume (Å^3)	r_{calc} (Å)	Ref
$P_3^{Si}Fe(N_2)$	881.2	5.9	8
$P_3^{Si}Fe(CN)$	1101.9	6.2	9
$P_3^{Si}Fe(CNMe)$	915.7	6.0	10
$P_3^{C}Fe(N_2)$	869.3	5.9	11
$P_3^{C}Fe(H)(N_2)$	869.8	5.9	9
$P_3^{B}Fe(NH_2)$	866.1	5.9	12
		Average	6.0 Å
		Std Dev	0.1 Å

5. Calculated Reorganization Energies

The inner-sphere reorganization energy for electron transfer ($\lambda_{is,ET}$) was estimated assuming non-adiabatic behavior and by calculating the difference between the single point energies of the relevant species in its ground state and the corresponding single point energy of this ground state in the oxidized or reduced geometry.

$$\lambda_{is,ET} = [E(Fe^{ox}{}_{ox}) - E(Fe^{ox}{}_{red})] + [E(Fe^{red}{}_{red}) - E(Fe^{red}{}_{ox})]$$

Relative reduction barriers were approximated by first defining the barrier for $P_3^BFe(NNH_2)^+$ to be 1.0 kcal/mol. Subsequent back-calculation of λ_{tot} yielded solutions of 30.5 kcal/mol and 56.5 kcal/mol, corresponding to the solutions in the inverted and normal regimes, respectively. The reorganization energy leading to the inverted solution would imply very small energies for KC_8 and solvent reorganization ($\lambda_{KC8} + \lambda_{OS} = 7.5$ kcal/mol). This led us to assume that the reduction steps were in the normal region. To check this assumption, outer-sphere reorganization energy was approximated using a continuum model.[13] For electron transfer ($\lambda_{os,ET}$) reactions the KC_8 reductant was modeled as an electrode surface ($r_{KC8} >> r_{cat}$). The radius of the P_3^EFe molecules (r_{cat}; Eq. 2) was approximated using the volumes of several relevant crystal structures. The values for the static and optical dielectric constant (ε_s and ε_{op}) of diethyl ether were taken as the values used in the SMD solvation model. This value was approximated at 33 kcal/mol, consistent with the reductions of interest occurring in the normal region. Accordingly, the total reorganization for $P_3^BFe(NNH_2)^+$ reduction ($G^* \equiv 1.0$ kcal/mol) was assumed to be 56.5 kcal/mol. Perturbation of this value by the differences between $\lambda_{IS}^{Si/C}$ and λ_{IS}^{B} lead to the relative barriers shown in **Table S3.**

Table S3. Summary of Calculated Reorganization Energies[a]

Redox Couple	$\lambda_{IS,ET}$	$\lambda_{OS} + \lambda_{KC8}$	G^*_{rel}
$P_3^BFe(NNH_2)^{+/0}$	23.0	33.5	1.0[b]
$P_3^{Si}Fe(NNH_2)^{+/0}$	29.7	33.5	4.4
$P_3^CFe(NNH_2)^{+/0}$	29.7	33.5	5.2

[a] All energies are in kcal/mol [b] G* values expressed relative to that of $P_3^BFe(NNH_2)^+$ reduction, defined as 1.0 kcal/mol

6. Determination of the Work Function

The work required to bring two cationic iron species together was approximated following the methods of Hammes-Schiffer and Mayer (Eq 1).[14]

$$w_r = \frac{e^2 Z_1 Z_2 f}{\epsilon_o r} \qquad \text{(eq. 1)}$$

Here Z_1 and Z_2 are the charges on each complex ($Z_1 = Z_2 = +1$) and e is the elementary charge. The distance between iron centers was taken as twice the radius of the P_3^EFe species (r = 12 Å) and ϵ_o is the static dielectric constant. The debye screening factor (f) was calculated using eq. 2.

$$f^{-1} = 1 + r\sqrt{\frac{8\pi N_A e^2 \mu}{10^{27}\epsilon_o k_B T}} \qquad \text{(eq. 2)}$$

Where μ is the ionic strength (taken as [Fe] = 1.3 mM) and N_A are k_B Avogadro's number and the Boltzmann constant, respectively. The temperature was taken as the standard temperature for catalysis (T =195 K). Substitution of the appropriate values into Eq. 1 and 2 yields w_r = 5.2 kcal/mol.

7. Summary of Wiberg Indices

Table S4. Summary of Wiberg Bond Indices for $P_3^EFe(N_2)$ complexes

P_3^BFe	Alpha	Beta	Total	$P_3^{Si}Fe$	Alpha	Beta	Total	P_3^CFe	Alpha	Beta	Total
Fe-N_1	0.2	0.2	0.9	Fe-N_1	0.2	0.3	1.0	Fe-N_1	0.2	0.3	1.0
Fe-N_2	0.1	0.1	0.4	Fe-N_2	0.1	0.1	0.4	Fe-N_2	0.1	0.1	0.4
N-N	0.7	0.6	2.6	N-N	0.6	0.6	2.6	N-N	0.6	0.6	2.5
Fe-B	0.1	0.1	0.4	Fe-Si	0.2	0.2	0.7	Fe-C	0.2	0.2	0.7
Fe-P_1	0.2	0.2	0.7	Fe-P_1	0.2	0.2	0.8	Fe-P_1	0.2	0.2	0.8
Fe-P_2	0.2	0.2	0.7	Fe-P_2	0.2	0.2	0.8	Fe-P_2	0.2	0.2	0.8
Fe-P_3	0.2	0.2	0.7	Fe-P_3	0.2	0.2	0.7	Fe-P_3	0.2	0.2	0.7

Table S5. Summary of Wiberg Bond Indices for $P_3^EFe(NNH)$ complexes

P_3^BFe	Alpha	Beta	Total	$P_3^{Si}Fe$	Alpha	Beta	Total	P_3^CFe	Alpha	Beta	Total
Fe-N_1	0.4	0.4	1.6	Fe-N_1	0.4	0.4	1.6	Fe-N_1	0.3	0.3	1.2
Fe-N_2	0.1	0.1	0.4	Fe-N_2	0.1	0.1	0.4	Fe-N_2	0.0	0.0	0.2
N-N	0.5	0.4	1.8	N-N	0.4	0.4	1.8	N-N	0.4	0.4	1.5
N-H	0.2	0.2	0.8	N-H	0.2	0.2	0.8	N-H	0.2	0.2	0.8
Fe-B	0.1	0.1	0.5	Fe-Si	0.2	0.2	0.7	Fe-C	0.1	0.1	0.5
Fe-P_1	0.2	0.2	0.7	Fe-P_1	0.2	0.2	0.8	Fe-P_1	0.2	0.2	0.7
Fe-P_2	0.2	0.2	0.8	Fe-P_2	0.2	0.2	0.8	Fe-P_2	0.2	0.2	0.8
Fe-P_3	0.2	0.2	0.8	Fe-P_3	0.2	0.2	0.8	Fe-P_3	0.2	0.2	0.7

Table S6. Summary of Bond Indices for $P_3^EFe(NNH_2)$ complexes

P_3^BFe	Alpha	Beta	Total	$P_3^{Si}Fe$	Alpha	Beta	Total	P_3^CFe	Alpha	Beta	Total
Fe-N_1	0.5	0.5	1.9	Fe-N_1	0.2	0.4	1.2	Fe-N_1	0.3	0.4	1.4
Fe-N_2	0.0	0.0	0.2	Fe-N_2	0.0	0.0	0.2	Fe-N_2	0.0		0.1
N-N	0.3	0.3	1.2	N-N	0.4	0.3	1.4	N-N	0.4	0.3	1.4
N-H	0.2	0.2	0.8	N-H	0.2	0.2	0.8	N-H	0.2	0.2	0.8
N-H	0.2	0.2	0.8	N-H	0.2	0.2	0.8	N-H	0.2	0.2	0.8
Fe-B	0.1	0.1	0.4	Fe-Si	0.2	0.2	0.7	Fe-C	0.1	0.1	0.5
Fe-P_1	0.2	0.2	0.8	Fe-P_1	0.2	0.2	0.8	Fe-P_1	0.2	0.2	0.8
Fe-P_2	0.2	0.2	0.8	Fe-P_2	0.2	0.2	0.8	Fe-P_2	0.2	0.2	0.8
Fe-P_3	0.2	0.2	0.8	Fe-P_3	0.2	0.2	0.8	Fe-P_3	0.2	0.2	0.8

Table S7. Summary of Wiberg Bond Indices for $P_3^EFe(N(4\text{-}OMe\text{-}Ph))$

P_3^BFe	Total
Fe-N_1	1.8
N-C	1.2
Fe-B	0.4
Fe-P_1	0.8
Fe-P_2	0.8
Fe-P_3	0.8

Table S8. Summary of Wiberg Bond Indices for C_2H_4 and C_2H_5

C_2H_4	Alpha	Beta	Total	C_2H_5	Alpha	Beta	Total
C_1-H_1	0.94	0.94	1.9	C_1-H_1	0.24	0.24	0.96
C_1-H_2	0.94	0.94	0.2	C_1-H_2	0.24	0.24	0.96
C_1-C_2	0.94	0.94	1.2	C_1-C_2	0.23	0.23	0.93
C_2-H_3	0.94	0.94	0.8	C_2-H_3	0.23	0.23	0.93
C_2-H_4	2.05	2.05	0.8	C_2-H_4	0.23	0.22	0.90
				C_2-H_5	0.27	0.28	1.10

8. Comparison of Calculated to Known Experimental Values

Table S9. Comparing of calculated to experimental values for several parameters of interest.

	Paramater	Calculated	Experimental	Ref
$P_3^{Si}Fe(NNMe_2)^+$	Singlet-Triplet Gap	6.9 kcal/mol	6.0	9
$P_3^{Si}Fe(NNMe_2)^+$	Reduction Potential	-1.81 V vs $Fc^{+/0}$	-1.73 V vs $Fc^{+/0}$	9
$P_3^{B}Fe(NNMe_2)$	Singlet-Triplet Gap	5.5 kcal/mol	4.0 kcal/mol	15
$P_3^{B}Fe(NNMe_2)$	Reduction Potential	-1.29 V vs $Fc^{+/0}$	-1.20 V vs $Fc^{+/0}$	14
$P_3^{Si}Fe(CNH)$	$BDFE_{N-H}$	43.5 kcal/mol	41.4 kcal/mol	9
$P_3^{Si}Fe(CNH)$	$BDFE_{N-H}$	61.8 kcal/mol	61.9 kcal/mol	9
$P_3^{Si}Fe(NNMeH)^+$	$BDFE_{N-H}$	45.9 kcal/mol	44.9 kcal/mol	9

9. References

[1] Grimme, S.; Antony, J.; Ehrlich, S.; Krieg, H. *J. Chem. Phys.* **2010**, *132*, 154104.
[2] Tao, J. M.; Perdew, J. P.; Staroverov, V. N.; Scuseria, G. E. *Phys. Rev. Lett.* **2003**, *91*, 146401.
[3] Weigend, F.; Ahlrichs, R. *Phys. Chem. Chem. Phys.* **2005**, *7*, 3297–3305.
[4] Towns, J. *et. al. Comput. Sci. Eng.* **2014***, 16,* 62-74.
[5] (a) Valiev, M.; Bylaska, E. J.; Govind, N.; Kowalski, K.; Straatsma, T. P.; Van Dam, H. J. J.; Wang, D.; Nieplocha, J.; Apra, E.; Windus, T. L.; de Jong, W. A. *Comput. Phys. Commun.* **2010**, *181*, 1477–1489. (b) Neese, F. *Wiley interdisciplinary Reviews - Computational Molecular Science*, **2012**, *2:1*, 73-78.
[6] (a) Klamt, A.; Schüürmann, G. *J. Chem. Soc. Perkin Trans. 2.* **1993**, *2,* 799–805. (b)Marten, B.; Kim, K.; Cortis, C.; Friesner, R. A.; Murphy, R. B.; Ringnalda, M. N.; Sitkoff, D.; Honig, B. *J. Phys. Chem.* **1996**, *100*, 11775–11788.
[7] Warren, J. J.; Tronic, T. A.; Mayer, J. M. *Chem. Rev.* **2010**, *110*, 6961–7001.
[8] Lee, Y.; Mankad, N. P.; Peters, J. C. *Nat. Chem.* **2010**, *2*, 558-565.
[9] Rittle, J.; Peters, J. C. *Angew. Chem. Int. Ed.* **2016**, *55*, 12262 –12265.
[10] Rittle, J.; Peters, J. C. *J. Am. Chem. Soc.* **2017**, *139*, 3161–3170.
[11] Creutz, S. E.; Peters, J. C. *J. Am. Chem. Soc.* **2014**, *136*, 1105−1115.
[12] Anderson, J. S.; Moret, M-. E.; Peters, J. C. *J. Am. Chem. Soc.* **2013**, *135*, 534−537.
[13] Marcus, R. A. *J. Chem. Phys.* **1956**, *24*, 966–978.
[14] (a) Iordanova, N.; Decornez, H.; Hammes-Schiffer, S. *J. Am. Chem. Soc.* **2001**, *123*, 3723-3733. (b) Roth, J. P.; Lovell, S.; Mayer, J. M. *J. Am. Chem. Soc.* **2000**, *122*, 5486-5498.
[15] Thompson, N. B.; Green, M. T.; Peters, J. C. *J. Am. Chem. Soc.* **2017**, *139*, 15312–15315.